Nanoscale Advances

ROYAL SOCIETY OF CHEMISTRY

PAPER

View Article Online
View Journal | View Issue

Cite this: *Nanoscale Adv.*, 2025, **7**, 4660

Self-assembled Ac-FFA-NH_2 based hydrogels with strong immunostimulating activity for vaccine delivery†

Nika Gazdek Serdar,[a] Tihomir Pospišil,[a] Marcela Šišić,[b] Ivo Crnolatac,[a] Petra Maleš,[a] Ruža Frkanec *[b] and Leo Frkanec *[a]

Recent research has demonstrated that peptide self-assemblies are effective as vaccine adjuvants, playing a critical role in enhancing vaccine efficacy. In our prior studies, the Ac-FFA-NH_2 peptide gelator was identified as a biocompatible material suitable for tissue engineering applications. In this study, we reveal that the self-assembled Ac-FFA-NH_2 hydrogel functions as a potent vaccine delivery system, as evidenced by its strong immunostimulatory activity *in vivo*. Mice vaccinated with OVA antigen incorporated into the hydrogel produced significantly higher IgG titers compared to both the unadjuvanted control group and those treated with traditional adjuvants. This suggests that the Ac-FFA-NH_2 hydrogel effectively induces a robust humoral immune response. Moreover, the hydrogel not only enhances humoral immunity but also stimulates a cellular immune response, as indicated by the production of the IgG2a subtype, further establishing it as an excellent vaccine delivery platform. Additionally, we describe a composite hydrogel developed through the stepwise self-assembly of the Ac-FFA-NH_2 peptide and liposomes. Structural characterization using TEM, DSC, and FTIR confirmed that both peptide nanofibers and lipid vesicles retain their structural integrity within the composite gel. Importantly, morphological analysis demonstrated that the mechanical robustness of the hydrogel remains largely unaffected by the presence of liposomes at lipid concentrations lower than the Ac-FFA-NH_2 concentration.

Received 9th January 2025
Accepted 13th June 2025

DOI: 10.1039/d5na00033e

rsc.li/nanoscale-advances

1. Introduction

The design and synthesis of safe and highly specific drug delivery systems with enhanced properties continue to be a top priority in the rapidly advancing field of nanomedicine.[1] Nanomedicine provides innovative platforms for drug delivery, which can significantly improve therapeutic efficacy while minimizing the toxicity associated with pharmaceuticals. A particularly promising advancement in this area is the use of supramolecular self-assembly nanomaterials, which rely on non-covalent interactions to offer several distinct advantages. These systems can undergo dynamic reorganization of their nano-structured morphologies and functions in response to specific stimuli, such as variations in pH, temperature, or ionic strength.[2–5] Among these, peptide-based self-assembling systems have emerged as especially noteworthy, drawing considerable attention in both materials science and biomedicine.[6,7] Peptide hydrogelators, primarily composed of natural amino acids, are biodegradable and easily metabolized by the body, making them highly suitable for therapeutic applications. Furthermore, supramolecular hydrogels, which are formed by the self-assembly of small molecules like low molecular weight hydrogelators (LMWHs), follow straightforward chemical synthesis routes to ensure high purity.[8] Their intrinsic biocompatibility, ease of functionalization, ability to form three-dimensional networks, and potential for controlled release of small molecules position them as particularly valuable for biomedical uses. These attributes are the focus of numerous reviews, which emphasize the importance of peptide-based systems in advancing drug delivery technologies.[9–11] Recent studies have further highlighted the potential of peptide-based nanomaterials as promising vaccine delivery systems, owing to their strong adjuvant activity and ability to trigger robust antibody responses.[12] Despite the success of conventional vaccine adjuvants, such as aluminum salts and oil-in-water emulsions, their use is often limited by safety concerns, inconsistent immune activation, or inability to elicit strong cellular responses.[13,14] Our research demonstrates that peptide-based self-assembling hydrogels can overcome these limitations by offering a biocompatible and tunable platform that promotes both humoral and cellular immune responses.

[a]*Division of Organic Chemistry and Biochemistry, Rudjer Bošković Institute, Bijenička 54, 10000 Zagreb, Croatia. E-mail: frkanec@irb.hr*

[b]*Centre for Research and Knowledge Transfer in Biotechnology, University of Zagreb, 10000 Zagreb, Croatia*

† Electronic supplementary information (ESI) available. See DOI: https://doi.org/10.1039/d5na00033e

Specifically, the Ac-FFA-NH_2 hydrogel supports balanced activation of Th1 and Th2 pathways—key to effective vaccine performance. These properties make it a promising candidate for next-generation vaccine adjuvants, with clear clinical relevance for infectious diseases and cancer immunotherapy. In our previous work, we demonstrated that the Ac-L-Phe-L-Phe-L-Ala-NH_2 (Ac-FFA-NH_2) hydrogel is biocompatible and supports the growth and proliferation of HEK293T cells within its gel fibers.[15] Continuing this line of research,[16] we focus on the synthesis and characterization of composite supramolecular hydrogels by combining Ac-FFA-NH_2 with liposomes. Incorporating lipid carriers such as liposomes into hydrogel formulations enables controlled drug or antigen release while enhancing bioavailability compared to plain hydrogels. Interactions between the hydrogelator and lipids can slow the release of molecules incorporated in both the liposomes and the hydrogel matrix. These interactions can also help stabilize the hydrogel and affect its degradation rate. The type and strength of these interactions depend on several factors, including the chemical structure and concentration of the phospholipids, as well as the chemical properties of the incorporated drugs.[17–22] However, many peptide-based hydrogel systems reported to date lack either *in vivo* immunological validation or tunable, sustained antigen release profiles—key requirements for effective vaccine delivery. To address this gap, we report a novel supramolecular system based on Ac-FFA-NH_2 that combines structural robustness, lipid-assisted controlled release, and *in vivo* immunostimulatory efficacy within a single platform. In this study, the model protein bovine serum albumin (BSA) was incorporated into the Ac-FFA-NH_2 hydrogel, and its effects on gelation properties, supramolecular self-assembly and protein release were studied. Small changes in the chemical structure and amino acid sequence of peptides can significantly influence the immunostimulatory properties of hydrogels.[23] Therefore, we synthesized several peptide analogs with slight structural modifications compared to Ac-FFA-NH_2, specifically Ac-FFA-OH, Ac-FFβA-OMe, and evaluated their immunostimulatory activities. This work presents, for the first time, a dual-function peptide–liposome hydrogel system with validated antigen delivery and immune-enhancing performance, highlighting its translational potential as a clinically relevant supramolecular vaccine platform. This research contributes to our ongoing efforts to develop potent immunostimulatory agents and innovative vaccine adjuvant delivery systems.[24,25]

2. Experimental section

2.1. Materials

All peptides and their precursors were synthesized, and detailed synthetic procedures along with full characterization are provided in the ESI (Schemes SI-1, and SI-2†). The gelator Ac-L-Phe-L-Phe-L-Ala-NH_2 (Ac-FFA-NH_2) and Ac-L-Phe-L-Phe-L-Ala-OH (Ac-FFA-OH) were synthesized following the previously optimized protocol.[15] Similarly, Ac-L-Phe-L-Phe-β-Ala-OMe (Ac-FFβA-OMe) was synthesized according to a reported procedure.[15] Cholesterol derived from porcine liver was obtained from Sigma (USA). L-α-Phosphatidylcholine (egg-PC), type XI-E, from fresh egg yolk, dipalmitoylphosphatidylcholine (DPPC), and dimyristoylphosphatidylcholine (DMPC) were purchased from Avanti Polar Lipids (USA). Bovine serum albumin (BSA) was sourced from Sigma Aldrich (Steinheim, Germany). Additional reagents, including Tween 20, monoclonal anti-chicken egg albumin (clone OVA-14, mouse IgG1 isotype), and *o*-phenylenediamine dihydrochloride, were also obtained from Sigma (USA). Horseradish-peroxidase-conjugated goat anti-mouse IgG (HRP-*anti*-mouse IgG) was supplied by Bio-Rad Laboratories (USA).

Biotin-conjugated rat anti-mouse IgG1 and IgG2a monoclonal antibodies, as well as streptavidin–peroxidase, were acquired from PharMingen, Becton Dickinson (USA). Chemicals used for buffers and solutions were purchased from Kemika (Croatia). Ovalbumin (OVA) was sourced from Serva (Germany). MilliQ ultrapure water was prepared using a Millipore Simplicity Ultrapure Water Purification System.

2.2. Synthesis of peptide hydrogelators

Following the method reported by Pospišil *et al.*, we synthesized the peptides Ac-FFA-NH_2 (**HYG-1**) and Ac-FFA-OH (**HYG-2**), although the initial yields were relatively low. After several attempts, a modified and more efficient four-step synthetic procedure was developed. Briefly, the starting compounds **1**, **2**, and **5** were prepared as described in previous reports.[26–28] The synthesis of compound **6** began with the preparation of dipeptide **3** through a standard DCC-mediated coupling reaction with compound **1**, yielding high conversion rates.[29] After the removal of the Boc protecting group, compound **4** was coupled with compound **5**. The resulting tripeptide **6** was synthesized using EDC/HOBt-mediated coupling.[30] Subsequent methyl ester to amide conversion produced Ac-L-Phe-L-Phe-L-Ala-NH_2 (**HYG-1**), while hydrolysis of the ester yielded Ac-FFA-OH (**HYG-2**) (Scheme SI-1†).Tripeptide Ac-FFβA-OMe (**HYG-3**) was synthesized *via* standard coupling procedures. This involved the preparation of protected dipeptides, followed by Boc group deprotection and further coupling to yield tripeptides, as detailed in the ESI (Schemes SI-1, and SI-2†). Deprotection of the Boc group followed by acetylation provided the final product, Ac-FFβA-OMe (**HYG-3**). All compounds were fully characterized using NMR, FTIR, and HRMS spectroscopy, with detailed spectral data provided in the ESI (Fig. SI-1–SI-21†).

2.3. Preparation of liposomes

Multilamellar liposomes were prepared using the thin lipid film method as described previously.[31] Briefly, egg-PC and cholesterol (molar ratio 3 : 2), DPPC, or DMPC were dissolved in a chloroform : methanol mixture (2 : 1) to a final lipid concentration of 30 mM. The solvent was evaporated under reduced pressure using a Rotavapor (Rotavapor® RE-121, Buchi), forming a thin lipid film. The dried lipid films were hydrated with 1 mL of phosphate buffer (PBS) or deuterium oxide (D_2O) for DSC measurements. The liposome suspensions were incubated overnight at 4 °C to allow swelling and stabilization. Liposome size was reduced by sequential extrusion of the multilamellar vesicles through polycarbonate membranes of 800, 400 and 200 nm, using a 0.5 mL extruder (LiposoFast, Avestin Inc., Canada).

Encapsulation of BSA or OVA into liposomes was performed by hydrating the preformed dry lipid films with solutions of BSA (3 mg mL^{-1} in PBS) or OVA (1 mg mL^{-1} in PBS).[32] The resulting liposome suspensions, without further separation of non-entrapped material, were used for immunization studies and for measuring the physicochemical properties of the liposomes.

2.4. Dynamic light scattering measurement (DLS)

The particle size distribution and zeta potential of the prepared liposomes were measured using a Zetasizer Nano US (Malvern, UK) equipped with a green laser (532 nm) following a previously described method.[33] The intensity of scattered light was detected at an angle of 173°, and measurements were performed at 25 °C. The data obtained were analyzed using Zetasizer software 6.20 (Malvern instruments). Liposome suspensions were diluted 10-fold in saline solution before analysis. The particle size of the liposomes is reported as the *z*-average diameter, calculated using Zetasizer Nano software based on the intensity of scattered light. Each sample was measured six times, and the results are presented as the mean value. For zeta potential measurements, liposomes were placed in specialized plastic cuvettes equipped with a gold electrode designed for zeta potential determination. Each sample was measured three times, and the results are expressed as the mean value.

2.5. Preparation of composite supramolecular hydrogel with liposomes

The hydrogelator Ac-FFA-NH_2 was dissolved in MilliQ water by heating until a clear solution was obtained. After slight cooling, and prior to gelation, preformed liposome suspensions (30 mM) at varying molar ratios were added to the solution. The composite hydrogel containing BSA-encapsulated liposomes was prepared following the same procedure, as detailed in ESI (Table S2†). BSA and FITC-BSA were dissolved in PBS and incorporated into the hydrogelator solutions following the same protocol. Gelation was confirmed using the inverted tube test (ESI, Table SI-1†).

2.6. Transmission electron microscopy

Structural and morphological characterization of the supramolecular composite hydrogel with liposomes and protein-loaded hydrogels was performed using a Zeiss EM 10A electron microscope at an acceleration voltage of 60 kV. A thin film of the gel was applied to a grid, followed by shading with palladium or contrasting with a 2% aqueous solution of the potassium salt of phosphotungstic acid (pWk, $H_3PW_{12}O_{40}$). The pWk solution was neutralized to pH 7 using NaOH, and a drop of this solution was placed on the gel sample. Excess solution was removed after 30 seconds.

2.7. Differential scanning calorimetry

Liposome suspensions of DPPC and DMPC for DSC measurements were prepared at a concentration of 7.5 mM. Samples of composite supramolecular hydrogels with Ac-FFA-NH_2 and liposomes were prepared as described in Section 2.5, with a final hydrogelator concentration of 17.56 mM. Before measurement, all samples were degassed under reduced pressure for 15 minutes. Calorimetric experiments were conducted using a Nano-DSC microcalorimeter (TA Instruments, New Castle, USA) at a scan rate of 1 °C min^{-1}. The temperature ranges were 10–60 °C for DPPC and 5–60 °C for DMPC, with a cell volume of 300 μL. Each sample was measured twice, including two independent fillings, across two heating and cooling cycles. The reference solution (MilliQ water) was scanned once under identical conditions, and its thermograms were subtracted from the raw sample data. Data were analysed using a Nano Analyze software package (TA Instruments).

2.8. FTIR-ATR

FTIR-ATR spectra were recorded using an INVENIO-S Bruker spectrometer equipped with a BioATR II unit and a photovoltaic LN-MCT detector. The KBr beam splitter was set at 1 mm, and the detector was operated at a scanner velocity of 15 kHz for high-sensitivity measurements. The ATR unit was purged with N_2 from an external supply. The BioATR II unit employs a circular dual crystal technology (DCT) design with an upper ATR crystal made of silicon and a lower crystal made of zinc selenide (ZnSe), the latter not in contact with the sample. The system provides multireflection performance with a path length of 6–8 μm and requires ~30 μL of sample.

The unit was temperature-controlled using a Huber Ministat 125 water bath set at 25 °C with a heating rate of 1 °C min^{-1}. Samples, including DPPC liposome suspensions, Ac-FFA-NH_2 hydrogel, and composite Ac-FFA-NH_2 hydrogels with liposomes in D_2O, were pipetted directly onto the ATR crystal in 25 μL volumes. Three independent sample replicates were prepared for each condition, along with a D_2O control at 25 °C. Spectra were collected at a resolution of 2 cm^{-1} with 128 scans per sample. Data acquisition, processing, and evaluation were performed using OPUS 8.5 SP1 software.

2.9. BSA release

For BSA release tests, both free BSA and liposome-encapsulated BSA were incorporated in hydrogels according to the procedure described in Experimental section 2.3. Briefly, multilamellar liposomes composed of egg-PC : Chol (in a molar ratio of 3 : 2) were prepared by the thin-lipid film method. BSA (3 mg mL^{-1}) in PBS was used for encapsulation. The size and charge of the prepared liposomes were determined by DLS prior to incorporation into the hydrogel. The prepared hydrogels were overlaid with 1.2 mL of PBS (pH 7.4) which was used as the release medium. Then, 600 μL of the release medium was taken out at different time intervals and replaced with fresh medium. Release studies were monitored for 83 hours. The concentration of released protein in the supernatant was measured using UV-vis spectrometry and calculated from a standard curve. The release efficiency was then calculated using the formula: release (%) = (released concentration)/(loaded concentration) × 100.

2.10. Mice and immunizations

Inbred NIH/OlaHsd mice were raised at the Institute of Immunology, Croatia. Female mice aged 2.0–2.5 months were

housed in the institute's Animal Facility with food and water provided ad libitum during the experiment. All animal experiments were conducted in accordance with the Croatian Law on Animal Welfare (2017) and the EC Directive 2010/63/EU. Ethical approval was obtained from the Ethical Committee of the Institute of Immunology and the Directorate of Veterinary and Food Safety of the Ministry of Agriculture, Republic of Croatia (approval number: HR-POK-009). Mice (five per group) were immunized subcutaneously at the tail base, followed by two booster doses, 21 days apart. Each injection volume was 0.1 mL, corresponding to 10 μg of OVA, 200 μg of PGM (control), 400 μg of hydrogelator, 0.30 μmol of MDP or imiquimod. Blood samples were collected on day seven after the final booster dose from the axillary plexus under anesthesia induced by intraperitoneal injection of ketamine/xylazine (25 mg kg^{-1} each). The sera were decomplemented at 56 °C for 30 minutes and stored at −20 °C until further analysis.

2.11. ELISA for quantitative determination of anti-OVA IgG

The levels of OVA-specific total IgG, IgG1, and IgG2a in mouse sera were quantified using ELISA as described previously.[34] High-binding ELISA plates (Costar, USA) were coated with 1.5 mg mL^{-1} OVA solution in carbonate buffer (pH 9.6) and incubated overnight at room temperature. Non-specific binding was blocked with 0.5% (w/v) BSA in PBS-T (0.05% (w/v) Tween 20 in PBS) for 2 h at 37 °C. Serial fivefold dilutions of mouse sera and standards were added in duplicate, followed by overnight incubation at room temperature. After washing, OVA-specific IgG levels were detected using HRP-conjugated goat anti-mouse IgG, incubated for 2 h at 37 °C. Plates were washed and developed with 0.6 mg mL^{-1} *o*-phenylenediamine dihydrochloride in citrate phosphate buffer (pH 5.0) containing 0.5 μL 30% H_2O_2/mL for 30 min in the dark. The reaction was stopped with 12.5% H_2SO_4, and absorbance was measured at 492 nm using a microplate reader (Thermo Fisher Scientific, Waltham, MA, USA). For IgG1 and IgG2a determination, biotin-conjugated rat anti-mouse IgG1 or IgG2a antibodies were incubated for 2 h at 37 °C, followed by streptavidin–peroxidase for an additional 2 h. The substrate solution was added and incubated as described above. Antibody subtype concentrations were quantified using parallel line assay with standard preparations of anti-OVA IgG (20 000 AU mL^{-1}), IgG1 (400 000 AU mL^{-1}), and IgG2a (5000 AU mL^{-1}).

2.12. Statistical analysis

Data were analyzed using Statistica 6.0 for Windows (StatSoft Inc.). Statistical significance was assessed using the Kruskal–Wallis test followed by *post hoc* comparisons. A p-value <0.05 was considered statistically significant.

3. Results and discussion

3.1. Peptide synthesis and composite supramolecular hydrogel preparation

Following the method reported by Pospišil *et al.*, we synthesized the peptides Ac-FFA-NH_2 and Ac-FFA-OH. However, the initial yields were relatively low, and extending the reaction time did not improve the yield. A modified, shortened four-step procedure was eventually developed, yielding higher amounts of the tripeptide. The structures of the new hydrogelators Ac-FFA-OH and Ac-FFβA-OMe were confirmed by ^{1}H NMR, with detailed chemical synthesis described in the ESI.†

Building on our previous findings that Ac-FFA-NH_2 supports HEK293T cell growth and proliferation within gel fibers,[15] we extended our research to composite supramolecular systems combining the hydrogelator with liposomes. The goal was to enhance the drug delivery performance of the hydrogel by incorporating liposomes, as previous studies have shown that liposomes can improve gel physical properties, enhance drug homogeneity, and enable sustained drug release from peptide hydrogels.[35,36] The literature also indicates the successful incorporation of liposomes loaded with bioactive substances into peptide hydrogels, with both lipid vesicles and peptide fibers retaining their structural integrity in the composite system.[37] Recent studies have highlighted the application of peptide hydrogels as vaccine adjuvant-delivery systems (VADS), demonstrating their strong adjuvant activity.[38,39] Based on these findings, we incorporated bovine serum albumin (BSA) and neutral multilamellar liposomes into the Ac-FFA-NH_2 hydrogel to evaluate the gel's properties and morphology. Testing revealed that the addition of liposomal suspensions with lipid concentrations 10, 5, and 2.5 times lower than the peptide gelator concentration resulted in the rapid formation of a cloudy white gel. However, at a lipid-to-gelator molar ratio of 1 : 1, no gel was formed (Table SI-1†). This aligns with prior studies showing that the size, surface chemistry, and quantity of liposomes significantly influence their interactions with hydrogelator molecules. As the liposome concentration in the nanocomposite hydrogel increases, the efficiency of cross-linking between hydrogelator molecules decreases.[40]

Furthermore, gel formation was delayed when BSA was added at concentrations ranging from 15–150 μg mg^{-1} of gelator. At lower protein concentrations, gel formation occurred within 30 minutes, while samples with 150 μg BSA per mg of gelator required overnight incubation to form a gel (Table S2†). Although our previous study showed that the Ac-L-Phe-L-Phe-L-Ala-NH_2 hydrogel can accommodate large biological entities, such as HEK293T cells,[15] high concentrations of BSA (>150 μg per mg of hydrogelator) were observed to inhibit gelation. FTIR and NMR analyses confirmed that hydrogel formation is driven by cross-β-sheet hydrogen bonding and other non-covalent interactions between tripeptide molecules. We therefore conclude that excessive BSA disrupts these specific interactions, interfering with the self-assembly and cross-linking processes required for stable gel network formation.

3.2. Morphological characterization of the composite hydrogel by TEM

To characterize the prepared nanocomposite supramolecular system, complementary microscopic and spectroscopic methods were employed.[41] Transmission electron microscopy (TEM) and confocal microscopy revealed the nanostructural

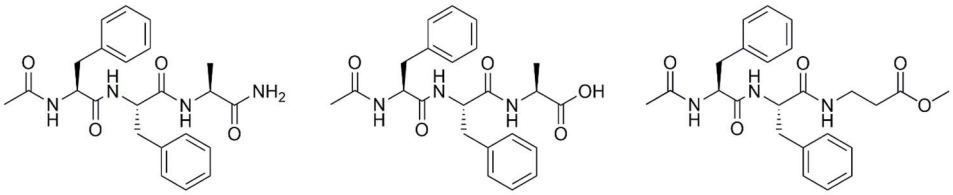

Fig. 1 Chemical structures of the synthesized hydrogelators: Ac-L-Phe-L-Phe-L-Ala-NH_2 (**HYG-1**); Ac-L-Phe-L-Phe-L-Ala-OH (**HYG-2**), Ac-L-Phe-L-Phe-βAla-OMe (**HYG-3**).

properties of the composite gel, confirming that Ac-FFA-NH_2 can self-assemble into a hydrogel in the presence of liposomes, BSA, and liposome-incorporated BSA (Fig. 2B–E and 3). TEM images of the nanofibrous hydrogel network revealed a mixture of fibers and straight ribbons, with diameters ranging from 50 to 500 nm and lengths extending into the micrometer range.[15] In hydrogel samples containing BSA, the hydrogel network preserved its structural integrity, but variations in fiber thickness were observed (Fig. 3). Confocal microscopy demonstrated the successful incorporation of FITC-BSA-loaded liposomes into the hydrogel, showing that liposomes do not impair the hydrogel network when lipid concentrations are lower than the Ac-FFA-NH_2 concentration. However, higher amounts of BSA resulted in slower gel formation or complete inhibition of gel formation.

3.3. Differential scanning calorimetry analysis of composite hydrogel (DSC)

Noncovalent interactions among peptide molecules drive the formation of assemblies and their subsequent transition into hydrogels. Interactions with phospholipid molecules in the lipid bilayer of liposomes can further influence both the lipid bilayer structure and hydrogel formation.[17,42] Differential scanning calorimetry (DSC) is a non-invasive physical technique that is well-suited for studying membrane bilayer phase transitions. It provides quantitative insights into how hydrogelator peptide molecules affect membrane structure and *vice versa*.[43] As peptides interact with lipids, they can alter various lipid properties, including packing, membrane fluidity, and cooperativity of phase transitions, which are reflected in the parameters measured during DSC experiments. Typically, the pre-transition phase is highly sensitive to molecules interacting with lipid headgroups and often disappears upon the addition of external molecules. In contrast, effects on the main phase transition indicate interactions at a deeper level, beyond the lipid headgroup region.[44] Multilamellar liposomes of DPPC and DMPC were prepared, and their size and charge were determined by dynamic light scattering (DLS) prior to DSC analysis.[45,46] The size of DPPC liposomes was 29 nm (±12 nm), while that of DMPC liposomes was 60 nm (±26 nm) (Table S1†). DMPC (14 : 0), a commonly used mammalian membrane mimetic, shows two endothermic transitions: a sharp main transition peak at

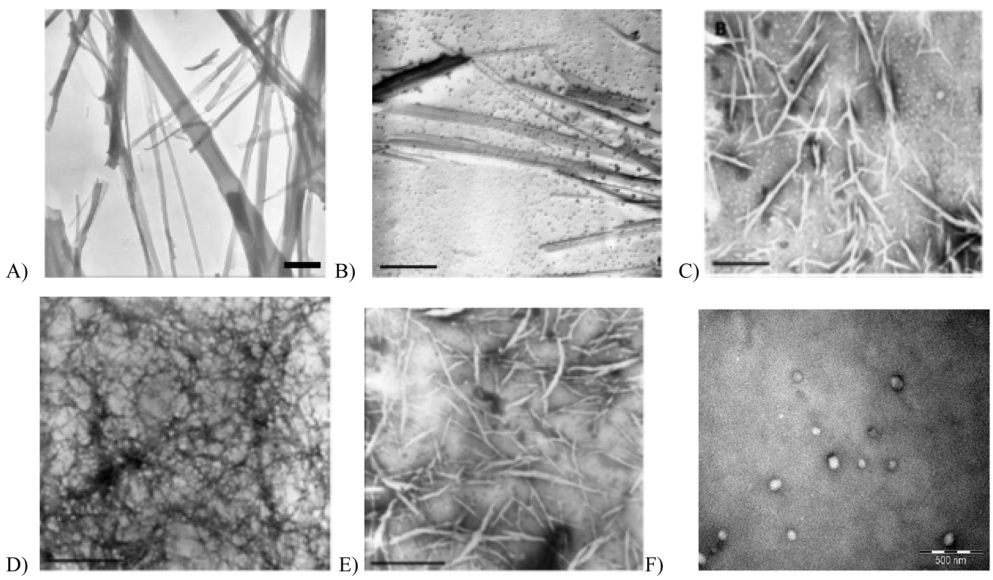

Fig. 2 TEM images of hydrogel (A) 0.4% (w/v) Ac-L-Phe-L-Phe-L-Ala-NH_2 in water. (B) Hydrogel with liposomes at a 5 : 1 molar ratio, stained with Pd. (C) Hydrogel with liposomes at a 5 : 1 ratio, stained with pWk; magnification 8000×. scale = 1 μm. (D) with BSA; (E) with liposome BSA; stained with pWk; magnification 160 00×. scale = 1 μm; (F) liposomes alone, scale = 500 nm.

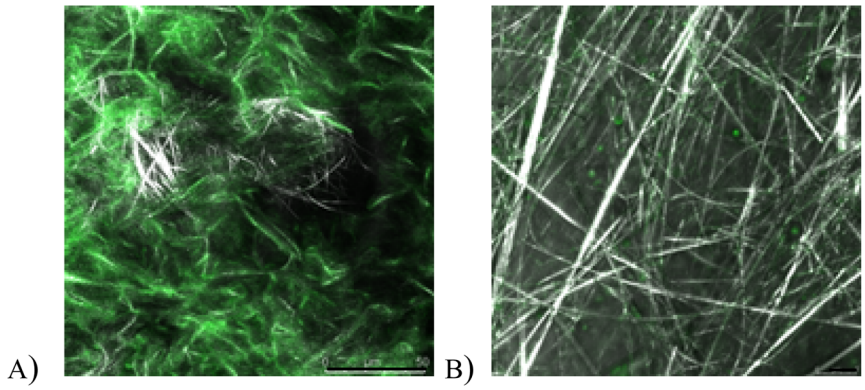

Fig. 3 Confocal images of the composite gel containing 0.4% (w/v) Ac-L-Phe-L-Phe-L-Ala-NH_2 in water: (A) with FITC-BSA, scale = 50 μm; (B) with liposome FITC-BSA, scale = 5 μm.

T_m = 24 °C and a broader pre-transition peak at $T_{pm1/2}$ = 11–15 °C. DPPC (16 : 0) has a main transition peak at T_m = 41 °C and a pre-transition peak at $T_{pm1/2}$ = 35 °C. DSC thermograms allow the extraction of three key parameters: Enthalpy of transition (ΔH), which is proportional to the area under the transition peak; ΔH reflects the strength of van der Waals forces between lipid fatty acid chains. Furthermore, full width at half maximum (FWHM or $\Delta T_{1/2}$), which indicates the cooperativity of the transition, related to the number of molecules transitioning simultaneously. Finally, transition temperatures (T_{pre}, T_m, and T_h) that correspond to the pre-transition, main phase transition, and other endothermic processes, respectively.[47] The results (Fig. 4) demonstrated that the addition of Ac-FFA-NH_2 to liposome suspensions affects the lipid bilayer in several ways. A slight shift and broadening of the main phase transition of phospholipids were observed, along with the disappearance of the pre-transition phase. Both the pre-transition and the main phase transition required less energy (ΔH) to initiate the rippled and liquid phases, respectively (Table 1). This suggests that interactions between Ac-FFA-NH_2 and lipid molecules destabilize the bilayer structure, consistent with the model proposed by Žinić *et al.*[48] According to this model, peptide self-assembly is primarily driven by hydrogen bonding, with Ac-FFA-NH_2 forming strong hydrogen bonds. The stacking structure is further stabilized by hydrophobic aromatic phenylalanine groups, which are known to significantly alter interfacial tension and surface domain morphology in DPPC films.[49]

Table 1 Phase transition temperature and transition enthalpies of liposomes and liposomal preparations with the Ac-FFA-NH_2 peptide hydrogelator, extracted from the DSC scans: temperature (T_m/°C), enthalpy (ΔH/kJ mol^{-1})

Sample	T_p/°C	ΔH/kJ mol^{-1}	T_m/°C	ΔH/kJ mol^{-1}
DPPC	34.93	2.92	41.78	22.40
Ac-FFA-NH_2: DPPC	32.98	1.38	41.33	11.72
DMPC	14.33	2.47	24.00	27.33
Ac-FFA-NH_2: DMPC	11.65	0.624	23.57	18.55

The obtained results revealed noticeable differences in the influence of hydrogelators on the shift and broadening of the main phase transition peak of DPPC or DMPC liposomal

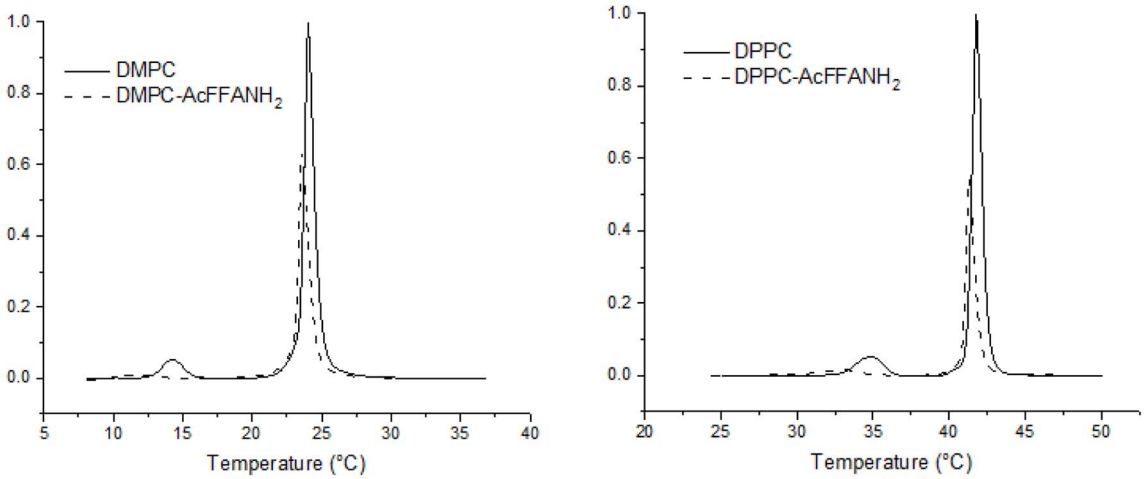

Fig. 4 Left: DSC thermograms, represented as baseline subtracted molar heat capacity traces of DPPC and Ac-FFA-NH_2 : DPPC in 2.5 : 1 ratio. Right: DSC Thermograms, represented as baseline subtracted molar heat capacity traces of DMPC and Ac-FFA-NH_2 : DMPC in 2.5 : 1 ratio.

bilayers as well as on enthalpy of the main transition (ΔH). ΔH is significantly lower for the main phase transition of DPPC when peptide is added in comparison with DMPC where the enthalpy was decreased but to lesser extent. The overall thermodynamic destabilization of the DPPC bilayer is prominent, exhibiting a twofold decrease in the enthalpy of the pre and main transition phases. The obtained results indicate stronger interactions of the Ac-FFA-NH_2 peptide with the inner part of the DPPC liposome bilayer. DPPC and DMPC are both zwitterionic lipids, with the only difference between them being the length of the fatty acid chain. The observed effect is likely due to differences in the packing of phospholipid molecules in the bilayer, resulting from fatty acid chain length and stronger hydrophobic interactions with hydrophobic phenylalanine. The stronger hydrophobic interaction of the peptide with DPPC can also be explained by the fact that the DPPC bilayer is more dehydrated and, therefore, more hydrophobic due to its higher phase transition temperature (41 °C) compared to that of DMPC (24 °C). On the other hand, peptide interactions with the membrane surface are accompanied by deformation of the surrounding lipid bilayer, affecting lipid packing and water penetration into the membrane, which would affect conformational changes of the membrane and enable peptide interactions with the interfacial hydrophobic regions of the DPPC bilayer (Fig. 5).[50]

Such extensive interference with the phospholipid conformation within bilayers indicates a strong and stable interaction, and its impact on adjuvant activity requires further detailed investigation.

3.4. FTIR-ATR analysis of the interaction between the Ac-FFA-NH_2 hydrogelator and phospholipids

The initial self-assembly of peptides occurs at the molecular level, and in mixtures of gelators, the molecules may either co-assemble or self-sort. Techniques such as infrared spectroscopy (FTIR), UV-vis absorption spectroscopy, fluorescence spectroscopy, and circular dichroism (CD) spectroscopy are valuable tools for probing molecular packing, hydrogen bonding, and other interactions.[41] The interaction between phospholipids in liposomes and the hydrogelator Ac-FFA-NH_2 was investigated using FTIR-ATR. All solutions were prepared in D_2O to mitigate the strong water absorption band at 3000–3600 cm^{-1}, which can obscure the detection of the CH_2 symmetric and antisymmetric stretches (2800–3000 cm^{-1}) from Ac-FFA-NH_2 and lipid components. The characteristic shape of the OH/NH stretching region provides insights into material hydration and hydrogen bonding.[51]

FTIR spectra were recorded for DPPC, Ac-FFA-NH_2, and their mixtures at 25 °C. Preprocessing of the spectral data included subtraction of the solvent (D_2O) spectrum and smoothing using the Savitsky–Golay filter (third-degree polynomial, 30 points). Baseline correction was applied to all spectra (full spectra available in the ESI, Fig. S8†). According to literature protocols,[52] analyses focused on specific spectral regions of interest: 3025–2825 cm^{-1}: CH_2 symmetric ($\nu_s CH_2$) and antisymmetric ($\nu_{as} CH_2$) stretching of methylene groups. 1775–1700 cm^{-1}: carbonyl group stretching (νCO). 1700–1567 cm^{-1}: amide I band (C═O stretching of secondary amides) and amide II band (NH_2 deformation of primary amides). The results revealed, in the CH_2 stretching region (3025–2825 cm^{-1}), that the spectral analysis of CH_2 stretching bands showed slight shifts in the band maxima upon the addition of Ac-FFA-NH_2 to DPPC liposomes. Specifically, the $\nu_{as} CH_2$ band shifted from 2923 cm^{-1} to 2931 cm^{-1}, while the $\nu_s CH_2$ band shifted from 2854 cm^{-1} to 2865 cm^{-1}. These shifts were accompanied by changes in band intensity. Such shifts suggest modifications in hydrogen bond distribution and possibly D–H replacement in the suspension.[53,54]

In the amide region (1700–1567 cm^{-1}): the amide I band at 1638 cm^{-1}, characteristic of Ac-FFA-NH_2, was also present in the Ac-FFA-NH_2 + DPPC mixture but, of course, absent in pure DPPC samples. The unchanged position of the 1638 cm^{-1} peak indicates that DPPC does not alter the secondary structure of Ac-FFA-NH_2. This observation suggests a non-destructive interaction between the peptide and lipid molecules, consistent with literature reports.[55]Carbonyl region (1775–1700 cm^{-1}): in the carbonyl stretching region, the addition of Ac-FFA-NH_2 to DPPC resulted only in intensity changes, indicating strong interactions between the peptide and the phospholipid

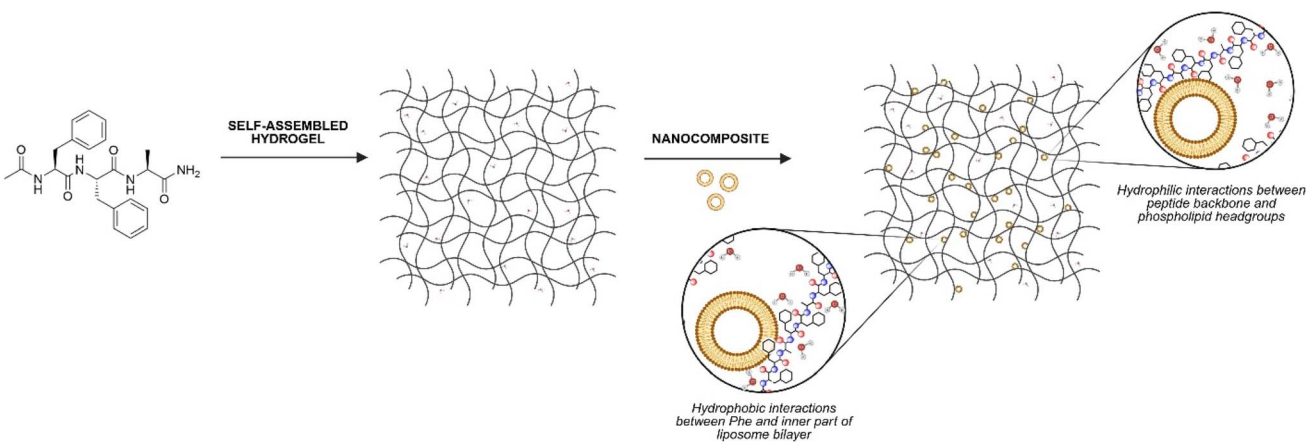

Fig. 5 Schematic presentation of the proposed interactions between liposomes and the Ac-FFA-NH_2 hydrogel.

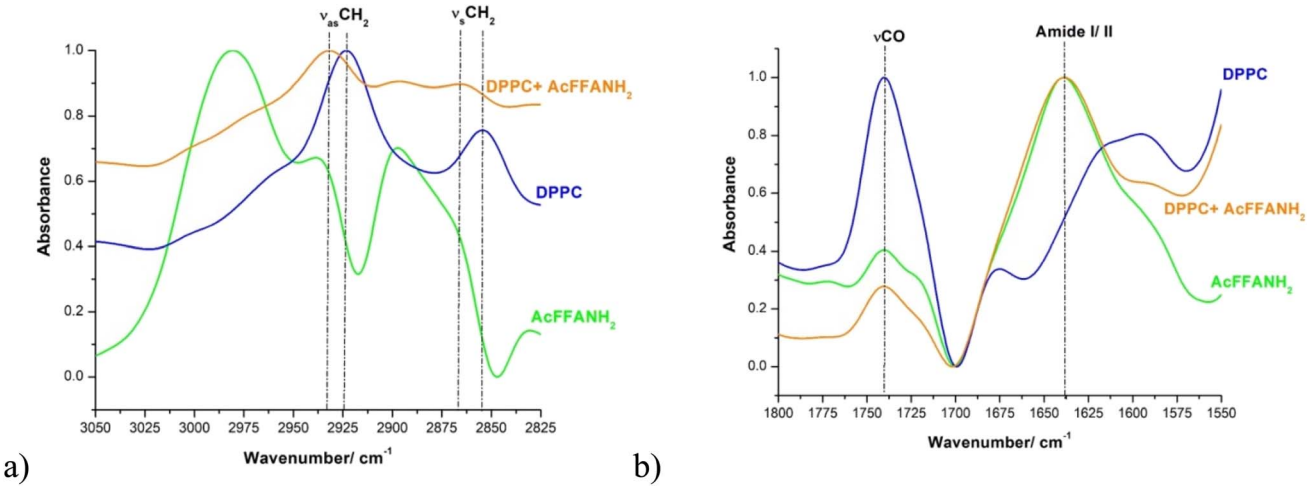

Fig. 6 Normalized FTIR spectra of (a) CH_2 stretching region marked with green (Ac-FFA-NH_2), blue (DPPC) and orange (DPPC + Ac-FFA-NH_2) lines. (b) νCO and amide band regions marked with green (Ac-FFA-NH_2), blue (DPPC) and orange (DPPC + Ac-FFA-NH_2) lines. The vertical lines show the maximum of the bands.

headgroups. This behavior aligns with findings from studies on antimicrobial peptides, where hydrophobic amino acids in peptides play a critical role in promoting deeper peptide insertion into lipid membranes.[56] The FTIR-ATR results (Fig. 6) demonstrate interactions between DPPC and the Ac-FFA-NH_2 peptide. The shifts and intensity changes in CH_2 and carbonyl bands imply modifications in lipid packing and peptide–lipid interactions. The findings support the hypothesis that liposomes are adsorbed onto the peptide fibrils within the supramolecular gel, as suggested in previous studies. These interactions likely contribute to the formation of a stable nanocomposite system with potential applications in drug delivery and other biomedical fields.

3.5. BSA release

The release kinetics of BSA were assessed by monitoring UV absorbance in the release medium overlying the hydrogels for 83 hours, under identical experimental conditions, enabling direct comparison of their release profiles (Fig. 7). The size of empty liposomes was 214.5 nm, while liposomes loaded with BSA measured 254.9 nm. Zeta-potential values were also measured: −11.6 mV for empty liposomes, and −6.9 mV for liposomes with encapsulated BSA. Non-encapsulated BSA was not separated from the liposomes, and the encapsulation efficiency was not directly measured. However, based on our previous work,[33] it was estimated to be approximately 30%. The concentration of BSA was kept constant in both samples to enable precise comparison between the two systems and ensure reliable absorbance values for the BSA released into the medium. Both hydrogel formulations—one containing free BSA and the other incorporating liposome-encapsulated BSA—exhibited a comparable initial burst phase, with 27.2% and 23.3% of BSA released within the first six hours, respectively. Discrete differences in release profiles were observed during this initial period. However, from the sixth hour onward, a clear

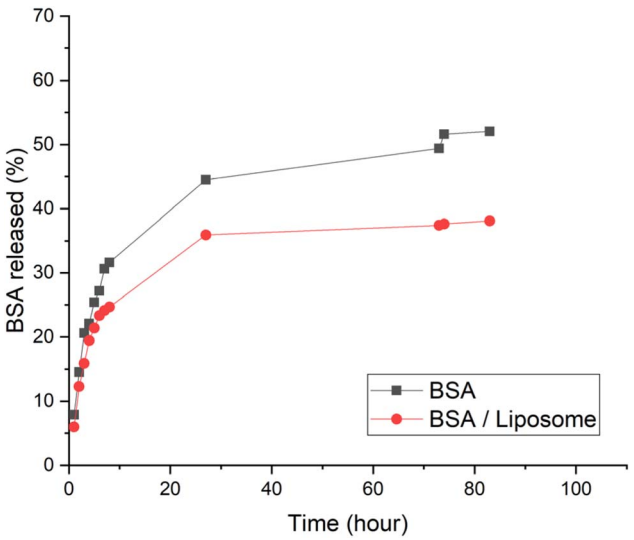

Fig. 7 Release kinetics of BSA and liposome-encapsulated BSA from the Ac-FFA-NH_2 hydrogel. 10 mM PBS (pH 7.4) was used as the release medium. BSA concentrations were measured using UV-vis spectrometry and calculated based on a standard calibration curve. Release efficiency was determined using the formula: release (%) = (released concentration/loaded concentration) × 100. Discrete differences in release profiles were observed during the initial period, with 27.2% and 23.3% of BSA released within the first six hours, for hydrogels containing free BSA and liposome-encapsulated BSA, respectively. However, beyond this period, the hydrogel containing liposome-encapsulated BSA exhibited a slower and more sustained release compared to the hydrogel with free BSA, with 52% release of free BSA and 38.1% release of liposome-encapsulated BSA after 83 hours.

divergence in release behavior became evident and persisted throughout the remainder of the study (Table SI-3†).

The hydrogel containing liposome-encapsulated BSA demonstrated a slower and more sustained release compared to the hydrogel containing free BSA. By the end of the 83-hour

period, 52% of free BSA and 38.1% of liposome-encapsulated BSA had been released. The comparable initial burst release observed in both hydrogel formulations is attributed to the rapid diffusion of free BSA: either directly incorporated into the hydrogel or originating from non-encapsulated BSA present in the hydrogel containing liposome-encapsulated BSA. In the later phase, the release profiles diverge: in the free BSA hydrogel, BSA slowly diffuses through the hydrogel matrix into the buffer, while in the hydrogel containing liposome-encapsulated BSA, the liposomal membranes further hinder release, leading to a more sustained release profile. The observed release profile for free BSA was consistent with similar published studies,[57] while the sustained release pattern of the liposome-encapsulated system highlights its potential as a biocompatible and effective platform for the controlled delivery of vaccine antigens.

3.6. *In vivo* testing of immunostimulating activity

The primary aim of this study was to evaluate the *in vivo* adjuvant activity of the synthesized peptide hydrogelators, focusing on the influence of their chemical structures. The chemical functionality of peptide hydrogels is crucial for their immunomodulatory properties. Research has demonstrated that even small alterations in the amino acid sequence, such as replacing hydrophobic residues or modifying the charge of functional groups, can greatly impact immunogenicity of peptide hydrogels.[12] The tested peptides are part of an extensive investigation of new supramolecular self-assembled nanomaterials. They differ at the N-terminal end, where α-alanine replaced is by β-alanine, and were selected for experiments (Fig. 1). The hydrogelators were assessed for their ability to induce specific immune responses, including total IgG production and the levels of IgG1 and IgG2a isotypes. A murine model of adjuvanticity was employed using ovalbumin (OVA) as a model antigen, following recommendation and a previously established immunization protocol.[58,59] ELISA and parallel-line analyses were conducted to quantify total anti-OVA IgG and its subclasses.

In addition to the hydrogelators, commercially available adjuvants with distinct modes of action were tested as positive controls. Our previous research demonstrated the adjuvant effects of peptidoglycan monomer (PGM), a bacterial-origin adjuvant,[59,60] while the immunostimulatory activities of muramyl dipeptide (MDP), liposomes, and the toll-like receptor 7/8 agonist imiquimod are also well-documented.[61–63] The efficacy of subunit vaccines often hinges on the strategic selection of adjuvants that can balance strong humoral and cellular immune responses. However, developing new adjuvants is a demanding and time-intensive process, reflected in the limited number of approved adjuvanted vaccines for human use.[64] A key requirement for preclinical testing of adjuvants is characterizing the immune response, including comparisons with well-known adjuvants. Our results revealed that the tested peptide hydrogelators induced strong and finely tuned systemic immune responses (Fig. 8).

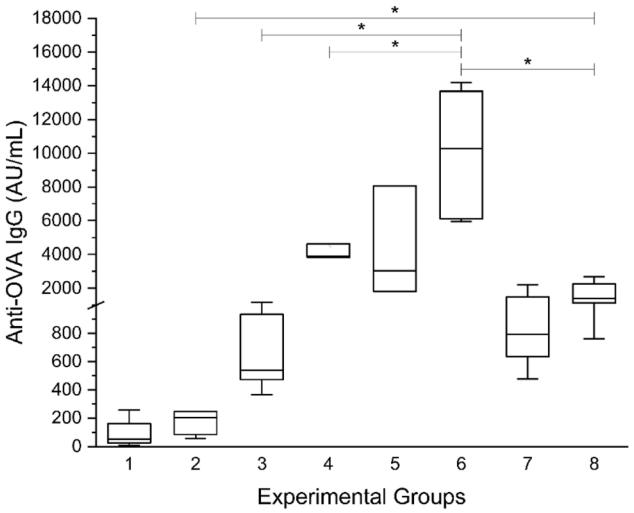

Fig. 8 The influence of adjuvants on production of total anti-OVA IgGs in mice sera: experimental groups: 1-OVA; 2-OVA + liposomes; 3-OVA + PGM; 4-OVA + MDP; 5-OVA + imiquimod; 6-OVA + Ac-FFA-NH_2; 7-OVA + Ac-FFβA-OMe; 8-OVA + Ac-FFA-OH; *$p < 0.05$ in comparison to the group connected with line.

Our key findings relate to total IgG production, subclass-specific responses and Th1/Th2 polarization. The highest total IgG antibody levels were observed in mice immunized with OVA incorporated into the Ac-FFA-NH_2 hydrogel, significantly exceeding those in mice immunized with OVA alone or with other adjuvants (Fig. 8). Ac-FFβA-OMe and Ac-FFA-OH hydrogelators induced less overall immune response compared to Ac-FFA-NH_2, but both produced significantly higher OVA-specific IgG titers than OVA alone or OVA formulated with liposomes or PGM. To further understand the immune response type, IgG1 (Th2-associated) and IgG2a (Th1-associated) isotypes were analyzed (Fig. 9). The Ac-FFA-NH_2 hydrogel, similar to MDP, significantly enhanced the production of IgG1 antibodies while also inducing IgG2a antibodies at levels comparable to imiquimod (Fig. 9a). In contrast, Ac-FFβA-OMe and Ac-FFA-OH hydrogels predominantly stimulated IgG2a production, suggesting a stronger Th1-mediated response (Fig. 9b).

The ratio of IgG1 to IgG2a in mice sera was used as an indirect marker for T-helper cell polarization (Th1 *vs.* Th2). Mice immunized with OVA + MDP and OVA + Ac-FFA-NH_2 displayed the highest IgG1/IgG2a ratios, indicating the ability of Ac-FFA-NH_2 to induce both humoral and cellular immune responses (Fig. 10). In contrast, the Ac-FFβA-OMe hydrogel shifted the immune reaction toward a Th1-dominant response.

The polarization of immunocompetent T cells into Th1 or Th2 pathways is critical for the immune response. Th1 cells promote cellular immunity, while Th2 cells drive humoral immunity and stimulate antibody production. The tested peptide hydrogelators demonstrated the ability to modulate immune responses, with Ac-FFA-NH_2 showing a balanced enhancement of both Th1- and Th2-associated pathways. The mechanisms of action behind adjuvant function at the molecular, cellular, and tissue levels are diverse and often not well

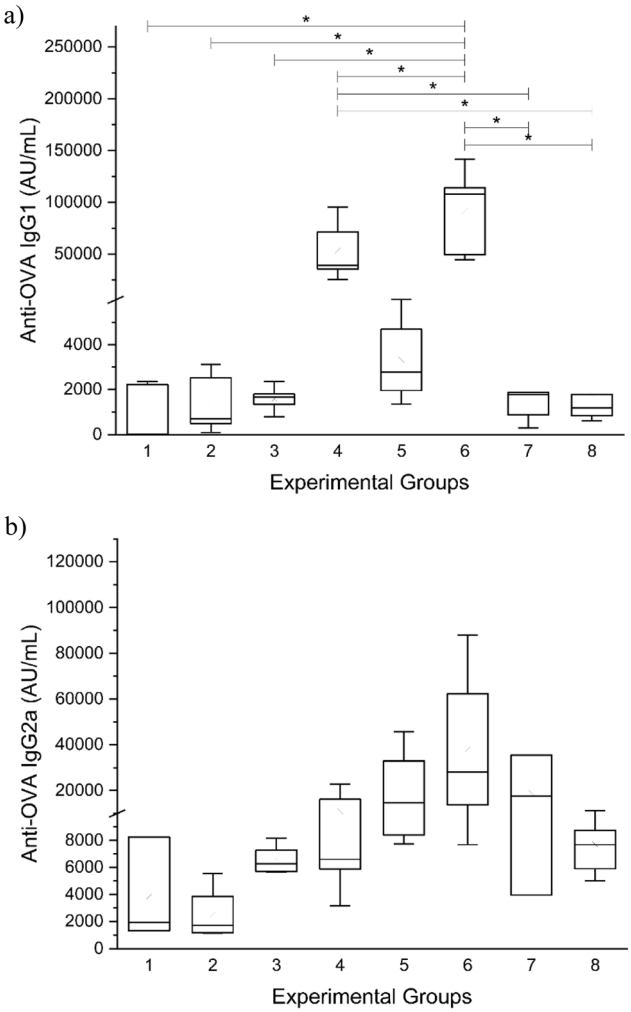

Fig. 9 The influence of adjuvants on production of immunoglobulins in mice: (a) anti-OVA IgG1; (b) anti-OVA IgG2a; experimental groups: 1-OVA; 2-OVA + liposomes; 3-OVA + PGM; 4-OVA + MDP; 5-OVA + imiquimod; 6-OVA + Ac-FFA-NH_2; 7-OVA + Ac-FFβA-OMe; 8-OVA + Ac-FFA-OH; *$p < 0.05$ in comparison to the group connected with line.

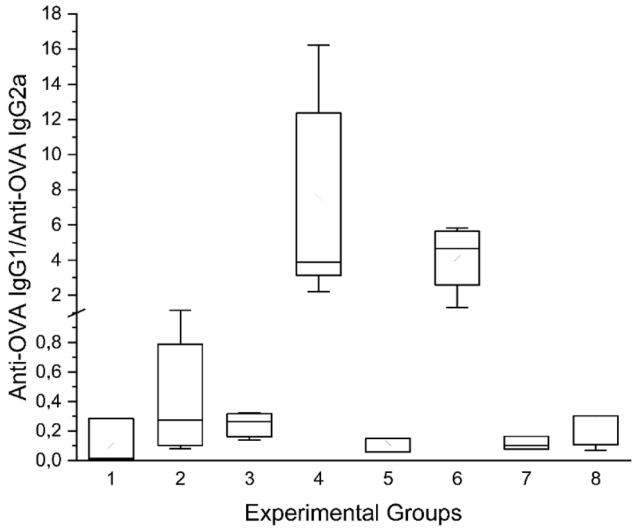

Fig. 10 Ratio of IgG1/IgG2a. Experimental groups: 1-OVA; 2-OVA + liposomes; 3-OVA + PGM; 4-OVA + MDP; 5-OVA + imiquimod; 6-OVA + Ac-FFA-NH_2; 7-OVA + Ac-FFβA-OMe; 8-OVA + Ac-FFA-OH.

understood. All adjuvants influence the immune response to coadministered antigens through complex and multifaceted mechanisms.[13,22] Peptide-based self-assembling nanomaterials primarily represent depot-forming adjuvants, where depot formation can lead to slow release of antigens at injection sites, immune cell recruitment to injection sites, and enhanced antigen uptake by APCs. Furthermore, the chemical structure of immunomodulators plays a pivotal role in activating the immune response. Even minor changes in the chemical functionality of molecules, such as modifications in the amino acid sequence or alterations in the charge of functional groups, can significantly affect immunogenicity. Supramolecular hydrogels[65,66] particularly the D-tetrapeptide Nap-GDFDFDY have previously shown superior immunostimulatory activity compared to alum. In these systems, substitution or repositioning of amino acids rapidly diminishes antibody titters in immunized mice. Peptides bearing protonated amines demonstrate stronger immune-stimulating activity than those with negatively charged, deprotonated carboxyl groups. The activation of cell-mediated immunity occurs through interactions between peptide hydrogelators and specific receptors on immunocompetent cells, such as antigen-presenting cells. The receptor affinity and the strength of the interaction depend on numerous factors, primarily the chemical structure, leading to the production of Th1- or Th2-type immune responses.[14] Our results demonstrate that the tested peptide hydrogels not only enhance antigen-specific immune responses but also modulate the balance between Th1 and Th2 pathways. This dual capability suggests the potential as novel, potent, and safe adjuvant systems for vaccine delivery. Further mechanistic studies are needed to fully elucidate the adjuvant action of these peptide hydrogels. It should be emphasized that this study highlights the exceptional immunostimulatory potential of the synthesized hydrogelators, particularly Ac-FFA-NH_2, which elicited both humoral and cellular immune responses. By leveraging their chemical versatility, these hydrogels hold promise for developing next-generation adjuvants for subunit vaccines.

4. Conclusions

The supramolecular self-assembly of tripeptides Ac-FFA-NH_2, Ac-FFβA-OMe, and Ac-FFA-OH was successfully achieved, and their immunostimulating activity was tested *in vivo*. Our results demonstrate that the tested hydrogels not only enhance antigen-specific immune responses but also modulate the direction of the immune reaction. Notably, immunization with Ac-FFA-NH_2 significantly increased the titers of total IgG, as well as IgG1 and IgG2a antibody isotypes, which serve as indicators of Th2 and Th1 immune responses, respectively. The observed effects were particularly pronounced for IgG2a, exceeding those elicited by well-known adjuvants such as liposomes and imiquimod. This resulted in a trend toward higher IgG1/IgG2a

ratios, indicating that Ac-FFA-NH_2 promotes a shift toward cellular immunity, in contrast to the predominantly Th2-polarized responses observed with unadjuvanted OVA. Furthermore, a nanocomposite hydrogel based on the stepwise self-assembly of the peptide Ac-FFA-NH_2 and liposomes was developed. The individual components of the self-assembled gel and the composite hydrogel were characterized using TEM, DSC, and FTIR, which revealed that peptide nanofibers and phospholipids in liposome vesicles interact discretely while maintaining their structural integrity within the composite gel. Importantly, the robustness of the hydrogel was largely unaffected by the presence of liposomes, provided their lipid concentrations remained lower than that of Ac-FFA-NH_2. The results revealed that the release rate of BSA from the hydrogel containing liposome-encapsulated BSA was slower than the release of BSA from the hydrogel alone. Such a biocompatible self-assembling supramolecular system, capable of sustained protein release, along with the ability to modulate immune responses and achieve a well-balanced enhancement of both Th1- and Th2-associated pathways, represents a very promising vaccine adjuvant-delivery system.

Data availability

The data supporting this article have been included as part of the ESI.†

Author contributions

Nika Gazdek Serdar: investigation, formal analysis, writing original draft, writing – review & editing. Marcela Šišić: investigation, formal analysis, writing – review & editing. Tomislav Pospišil: methodology, investigation. Ivo Crnolatac: methodology, investigation, writing – review & editing. Petra Maleš: methodology, investigation. Ruža Frkanec: conceptualization, supervision, methodology, writing – review & editing. Leo Frkanec: conceptualization, supervision, methodology, funding acquisition, writing – review & editing, writing – original draft.

Conflicts of interest

The authors declare no conflict of interest.

Acknowledgements

This research was funded by the Croatian Science Foundation, project HRZZ-IP-2018-01-6910, and by the Ministry of Science and Education of the Republic of Croatia. We would like to thank the Croatian Science Foundation for financial support of the project "Synthesis of supramolecular self-assembled nanostructures for the construction of advanced functional materials (SUPeRNANO)", HRZZ-IP-2018-01-6910 and the Ministry of Science and Education of Republic of Croatia, for financial support of the project "Development of Composite Hydrogel based on Self-assembled Peptides and Poly(vinyl alcohol) for Regeneration and Replacement of Articular Cartilage". The authors acknowledge the HRZZ IP-2020-02-7669 project for providing access to the INVENIO-S Bruker spectrometer equipped with a BioATR II unit. The authors would like to thank Lucija Horvat for TEM analysis of the hydrogel samples, dr Mario Cindrić and dr. Marijana Erk for HRMS analysis and Professor Ernest Meštrović for his help in editing the manuscript.

References

1 M. Puccetti, M. Pariano, A. Schoubben, S. Giovagnoli and M. Ricci, Biologics, theranostics, and personalized medicine in drug delivery systems, *Pharmacol. Res.*, 2024, **201**, 107086.
2 B. Rybtchinski, Adaptive supramolecular nanomaterials based on strong noncovalent interactions, *ACS Nano*, 2011, **5**, 6791–6818.
3 K. Liu, Y. Kang, Z. Wang and X. Zhang, 25th anniversary article: reversible and adaptive functional supramolecular materials: "noncovalent interaction" matters, *Adv. Mat.*, 2013, **25**, 5530–5548.
4 L. Adler-Abramovich and E. Gazit, The physical properties of supramolecular peptide assemblies: from building block association to technological applications, *Chem. Soc. Rev.*, 2014, **43**, 6881–6893.
5 S. La Manna, C. Di Natale, V. Onesto and D. Marasco, Self-Assembling Peptides: From Design to Biomedical Applications, *Int. J. Mol. Sci.*, 2021, **22**(23), 12662.
6 V. P. Conticello, Peptide-based nanomaterials: Building back better & beyond, *Curr. Opin. Solid State Mater. Sci.*, 2023, **27**(2), 101066.
7 Y. Hua and Y. Shen, Applications of self-assembled peptide hydrogels in anti-tumor therapy, *Nanoscale Adv.*, 2024, **6**, 2993–3008.
8 Y. Kuang, N. Zhou and B. Xu, *Biocompatibility of Hydrogelators Based on Small Peptide Derivatives in Hydrogels in Cell-Based Therapies*, ed. C. J. Connon and I. W. Hamley, The Royal Society of Chemistry, 2014, ch. 2, pp. 31–47.
9 Y. Wang, W. Zhang, C. Gong, B. Liu, Y. Li, L. Wang, Z. Su and G. Wei, Recent advances in the fabrication, functionalization, and bioapplications of peptide hydrogels, *Soft Matter*, 2020, **16**, 10029–10045.
10 C. Wu, W. Liao, Y. Zhang and Y. Yan, Peptide-based supramolecular hydrogels and their biotherapeutic applications, *Biomater. Sci.*, 2024, **12**, 4855–4874.
11 E. Gallo, C. Diaferia, E. Rosa, G. Smaldone, G. Morelli and A. Accardo, Peptide-Based Hydrogels and Nanogels for Delivery of Doxorubicin, *Int. J. Nanomed.*, 2021, **16**, 1617–1630.
12 T. L. Lopez-Silva, D. G. Leach, A. Azares, I. C. Li, D. G. Woodside and J. D. Hartgerink, Chemical functionality of multidomain peptide hydrogels governs early host immune response, *Biomaterials*, 2020, **231**, 119667.
13 E. Ben-Akiva, A. Chapman, T. Mao and D. J. Irvine, Linking vaccine adjuvant mechanisms of action to function, *Sci. Immunol.*, 2025, **14**, eado5937.

14 T. Zhao, Y. Cai, Y. Jiang, X. He, Y. Wei, Y. Yu and X. Tian, Vaccine adjuvants: mechanisms and platforms, *Signal Transduction Targeted Ther.*, 2023, **8**, 283.
15 T. Pospišil, L. Ferhatovic Hamzic, L. Brkic Ahmed, M. Lovric, S. Gajovic and L. Frkanec, Synthesis, characterization and *in vitro* biocompatibility assessment of a novel tripeptide hydrogelator, as a promising scaffold for tissue engineering applications, *Biomater. Sci.*, 2016, **4**, 1412–1416.
16 T. Gregorič, J. Makarević, Z. Štefanić, M. Žinič and L. Frkanec, Gamma Radiation- and Ultraviolet Induced Polymerization of Bis(aminoacid)fumaramide Gel Assemblies, *Polymers*, 2022, **14**, 214.
17 J. Boekhoven, A. M. Brizard, M. C. A. Stuart, L. Florusse, G. Raffy, A. Del Guerzo and J. H. van Esch, Bio-inspired supramolecular materials by orthogonal self-assembly of hydrogelators and phospholipids, *Chem. Sci.*, 2016, **7**, 6021–6031.
18 S. Grijalvo, J. Mayr, R. Eritja and D. D. Diaz, Biodegradable liposome-encapsulated hydrogels for biomedical applications: a marriage of convenience, *Biomater. Sci.*, 2016, **4**, 555–574.
19 M. M. Ibrahim, A. B. Nair, B. E. Aldhubiab and T. M. Shehata, Hydrogels and Their Combination with Liposomes, Niosomes, or Transfersomes for Dermal and Transdermal Drug Delivery, in *Liposomes*, ed. A. Catala, Intechopen, 2017, DOI: **10.5772/intechopen.68158**.
20 Y. Wang, Z. Xu, M. Lovrak, V. A. A. le Sage, K. Zhang, X. Guo, R. Eelkema, E. Mendes and J. H. van Esch, Biomimetic Strain-Stiffening Self-Assembled Hydrogels, *Angew. Chem.*, 2020, **59**, 4830–4834.
21 M. W. Joraholmen, M. Johannessen, K. Gravningen, M. Puolakkainen, G. Acharya, P. Basnet and N. Skalko-Basnet, Liposomes-In-Hydrogel Delivery System Enhances the Potential of Resveratrol in Combating Vaginal Chlamydia Infection, *Pharmaceutics*, 2020, **12**(12), 1203.
22 N. C. Wickremasinghe, V. A. Kumar and J. D. Hartgerink, Two-step self-assembly of liposome-multidomain peptide nanofiber hydrogel for time-controlled release, *Biomacromolecules*, 2014, **15**, 3587–3595.
23 Y. Zhang, Z. Hu, X. Li, Y. Ding, Z. Zhang, X. Zhang, W. Zheng and Z. Yang, Amino acid sequence determines the adjuvant potency of a D-tetra-peptide hydrogel, *Biomater. Sci.*, 2022, **10**, 3092–3098.
24 S. Guzelj, M. Weiss, B. Slütter, R. Frkanec and Ž. Jakopin, Covalently Conjugated NOD2/TLR7 Agonists Are Potent and Versatile Immune Potentiators, *J. Med. Chem.*, 2022, **65**(22), 15085–15101.
25 S. Guzelj, M. Šišić, Š. Bizjak, L. Frkanec, R. Frkanec and Ž. Jakopin, Lipidation of NOD2 Agonists with Adamantane And Stearoyl Moieties Differentially Regulates Their *In Vivo* Adjuvant Activity, *Pharmaceutics*, 2022, **14**(12), 2755.
26 O. Keller, W. E. Keller, G. v. Look and G. Wersin, *tert*-Butoxycarbonylation of Amino Acids and their Derivatives:*N-tert*-Butoxycarbonyl-l-phenylalanine, in *Organic Syntheses*, Wiley, 2003, vol. 63, p. 160.
27 J. Li and Y. Sha, A convenient synthesis of amino acid methyl esters, *Molecules*, 2008, **13**, 1111–1119.
28 J. G. Nathanael, L. F. Gamon, M. Cordes, P. R. Rablen, T. Bally, K. M. Fromm, B. Giese and U. Wille, Amide Neighbouring-Group Effects in Peptides: Phenylalanine as Relay Amino Acid in Long-Distance Electron Transfer, *ChemBioChem*, 2018, **19**, 922–926.
29 A. Banerjee, G. Palui and A. Banerjee, Pentapeptide based organogels: the role of adjacently located phenylalanine residues in gel formation, *Soft Matter*, 2008, **4**, 1430–1437.
30 L. Marchetti and B. DeBoef, Solution-Phase Synthesis of Dipeptides: A Capstone Project That Employs Key Techniques in an Organic Laboratory Course, *J. Chem. Educ.*, 2015, **92**(9), 1536–1538.
31 R. Frkanec, D. Travas, M. Krstanovic, B. H. Spoljar, D. Ljevakovic, B. Vranesic, L. Frkanec and J. Tomasic, Entrapment of peptidoglycans and adamantyltripeptides into liposomes: an HPLC assay for determination of encapsulation efficiency, *J. Liposome Res.*, 2003, **13**, 279–294.
32 R. Frkanec, V. Noethig-Laslo, B. Vranešić, K. Mirosavljević and J. Tomašić, A spin labelling study of immunomodulating peptidoglycan monomer and adamantyltripeptides entrapped into liposomes, *Biochim. Biophys. Acta, Biomembr.*, 2003, **1611**, 187–196.
33 M. Brgles, D. Jurasin, M. D. Sikiric, R. Frkanec and J. Tomasic, Entrapment of ovalbumin into liposomes-factors affecting entrapment efficiency, liposome size, and zeta potential, *J. Liposome Res.*, 2008, **18**, 235–248.
34 L. Habjanec, R. Frkanec, B. Halassy and J. Tomasic, Effect of liposomal formulations and immunostimulating peptidoglycan monomer (PGM) on the immune reaction to ovalbumin in mice, *J. Liposome Res.*, 2006, **16**, 1–16.
35 M. Sanati and S. A. Yavari, Liposome-integrated hydrogel hybrids: Promising platforms for cancer therapy and tissue regeneration, *J. Controlled Release*, 2024, **368**, 703–727.
36 J. W. R. Swain, C. Y. Yang and Y. D. Hartgerink, Orthogonal Self-Assembly of Amphiphilic Peptide Hydrogels and Liposomes Results in Composite Materials with Tunable Release Profiles, *Biomacromolecules*, 2023, **24**(11), 5018–5026.
37 J. Hurler, S. Zakelj, J. Mravljak, S. Pajk, A. Kristl, R. Schubert and N. Skalko-Basnet, The effect of lipid composition and liposome size on the release properties of liposomes-in-hydrogel, *Int. J. Pharm.*, 2013, **456**, 49–57.
38 Z. Luo, Q. Wu, C. Yang, H. Wang, T. He, Y. Wang, Z. Wang, H. Chen, X. Li, C. Gong and Z. Yang, A Powerful CD8(+) T-Cell Stimulating D-Tetra-Peptide Hydrogel as a Very Promising Vaccine Adjuvant, *Adv. Mater.*, 2017, **29**(5), 1601776.
39 X. Wu, S. Tang, Z. Wang, X. Ma, L. Zhang, F. Zhang, L. Xiao, S. Zhao, Q. Li, Y. Wang, Q. Wang and K. Chen, Immune Enhancement by the Tetra-Peptide Hydrogel as a Promising Adjuvant for an H7N9 Vaccine against Highly Pathogenic H7N9 Virus, *Vaccines*, 2022, **10**(1), 130.
40 S. Correa, A. K. Grosskopf, J. H. Klich, H. L. Hernandez and E. A. Appel, Injectable Liposome-based Supramolecular Hydrogels for the Programmable Release of Multiple Protein Drugs, *Matter*, 2022, **5**(6), 1816–1838.

41 E. R. Draper and D. J. Adams, How Should Multicomponent Supramolecular Gels Be Characterised?, *Chem. Soc. Rev.*, 2018, **47**, 3395–3405.
42 G. Duché, C. Heu and P. Thordarson, Development and Characterization of Nanoscale Gel-Core Liposomes Using a Short Self-Assembled Peptide Hydrogel: Implications for Drug Delivery, *ACS Appl. Nano Mater.*, 2023, **6**, 14745–14755.
43 R. N. Lewis, D. A. Mannock and R. N. McElhaney, Differential scanning calorimetry in the study of lipid phase transitions in model and biological membranes: practical considerations, *Methods Mol. Biol.*, 2007, **400**, 171–195.
44 M. L. Jobin and I. D. Alves, The Contribution of Differential Scanning Calorimetry for the Study of Peptide/Lipid Interactions, *Methods Mol. Biol.*, 2019, **1964**, 3–15.
45 P. F. Almeida, F. E. Carter, K. M. Kilgour, M. H. Raymonda and E. Tejada, Heat Capacity of DPPC/Cholesterol Mixtures: Comparison of Single Bilayers with Multibilayers and Simulations, *Langmuir*, 2018, **34**, 9798–9809.
46 M. A. Morini, M. B. Sierra, V. I. Pedroni, L. M. Alarcon, G. A. Appignanesi and E. A. Disalvo, Influence of temperature, anions and size distribution on the zeta potential of DMPC, DPPC and DMPE lipid vesicles, *Colloids Surf., B*, 2015, **131**, 54–58.
47 C. Demetzos, Differential Scanning Calorimetry (DSC): a tool to study the thermal behavior of lipid bilayers and liposomal stability, *J. Liposome Res.*, 2008, **18**, 159–173.
48 J. Makarević, M. Jokić, B. Perić, V. Tomišić, B. Kojić-Prodić and M. Žinić, Bis(Amino Acid) Oxalyl Amides as Ambidextrous Gelators of Water and Organic Solvents: Supramolecular Gels with Temperature Dependent Assembly/Dissolution Equilibrium, *Chem.–Eur. J*, 2001, **7**, 3328–3341.
49 E. C. Griffith, R. J. Perkins, D. M. Telesford, E. M. Adams, L. Cwiklik, H. C. Allen, M. Roeselová and V. Vaida, Interaction of L-Phenylalanine with a Phospholipid Monolayer at the Water-Air Interface, *J. Phys. Chem. B*, 2015, **119**(29), 9038–9048.
50 A. Garcia, H. Zou, K. R. Hossain, Q. H. Xu, A. Buda and R. J. Clarke, Polar Interactions Play an Important Role in the Energetics of the Main Phase Transition of Phosphatidylcholine Membranes, *ACS Omega*, 2019, **4**(1), 518–527.
51 B. de Campos Vidal and M. L. S. Mello, Collagen type I amide I band infrared spectroscopy, *Micron*, 2011, **42**, 283–289.
52 M. Foggia, P. Taddei, A. Torreggiani, M. Dettin and A. Tinti, Self-assembling peptides for biomedical applications: IR and Raman spectroscopies for the study of secondary structure, *Proteomics Res. J.*, 2012, **2**, 231–272.
53 C. Jiang, A. Gamarnik and C. P. Tripp, Identification of lipid aggregate structures on TiO_2 surface using headgroup IR bands, *J. Phys. Chem. B*, 2005, **109**, 4539–4544.
54 E. Y. Jiang and J. Rieppo, Enhancing FTIR imaging capabilities with two-dimensional correlation spectroscopy (2DCOS): a study of concentration gradients of collagen and proteoglycans in human patellar cartilage, *J. Mol. Struct.*, 2006, **799**, 196–203.
55 P. Chakraborty, M. Ghosh, L. Schnaider, N. Adadi, W. Ji, D. Bychenko, T. Dvir, L. Adler-Abramovich and E. Gazit, Composite of Peptide-Supramolecular Polymer and Covalent Polymer Comprises a New Multifunctional, Bio-Inspired Soft Material, *Macromol. Rapid Commun.*, 2019, **40**, e1900175.
56 R. Oliva, M. Chino, K. Pane, V. Pistorio, A. De Santis, E. Pizzo, G. D'Errico, V. Pavone, A. Lombard, P. Del Vecchio, E. Notomista, F. Nastri and L. Petraccone, Exploring the role of unnatural amino acids in antimicrobial peptides, *Sci. Rep.*, 2018, **8**(1), 8888.
57 K. Roy, G. Pandit, M. Chetia, A. K. Sarkar, S. Chowdhuri, A. P. Bidkar and S. Chatterjee, Peptide Hydrogels as Platforms for sustained Release of Antimicrobial and Antitumor Drugs and Proteins, *ACS Appl. Bio Mater.*, 2020, **3**, 6251–6262.
58 D. E. S. Stewart-Tull, Recommendations for the Assessment of Adjuvants (Immunopotentiators), in *Immunological Adjuvants and Vaccines*, ed. G. Gregoriadis, A. C. Allison and G. Poste, NATO ASI Series, NSSA, vol. 179, Springer, Boston, MA, 1989, pp. 213–226.
59 L. Habjanec, R. Frkanec, B. Halassy and J. Tomašić, Effect of liposomal formulations and immunostimulating peptidoglycan monomer (PGM) on the immune reaction to ovalbumin in mice, *J. Liposome Res.*, 2006, **16**, 1–16.
60 B. Halassy, M. Krstanovic, R. Frkanec and J. Tomasic, Adjuvant activity of peptidoglycan monomer and its metabolic products, *Vaccine*, 2003, **21**, 971–976.
61 F. Ellouz, A. Adam, R. Ciorbaru and E. Lederer, Minimal structural requirements for adjuvant activity of bacterial peptidoglycan derivatives, *Biochem. Biophys. Res. Commun.*, 1974, **59**, 1317–1325.
62 Y. Perrie, F. Crofts, A. Devitt, H. R. Griffiths, E. Kastner and V. Nadella, Designing liposomal adjuvants for the next generation of vaccines, *Adv. Drug Deliv. Rev.*, 2016, **99**, 85–96.
63 J. P. Vasilakos and M. A. Tomai, The use of Toll-like receptor 7/8 agonists as vaccine adjuvants, *Expert Rev. Vaccines*, 2013, **12**, 809–819.
64 E. Nanishi, D. J. Dowling and O. Levy, Toward precision adjuvants: optimizing science and safety, *Curr. Opin. Pediatr.*, 2020, **32**, 125–138.
65 E. C. Gale, A. E. Powell, G. A. Roth, E. L. Meany, J. Yan, B. S. Ou, A. K. Grosskopf, J. Adamska, V. Picece, A. I. d'Aquino, B. Pulendran, P. S. Kim and E. A. Appel, Hydrogel-Based Slow Release of a Receptor-Binding Domain Subunit Vaccine Elicits Neutralizing Antibody Responses Against SARS-CoV-2, *Adv. Mater.*, 2021, **33**, e2104362.
66 N. Falcone, M. Ermis, D. Goksu Tamay, M. Mecwan, M. Monirizad, T. Grett Mathes, V. Jucaud, A. Choroomi, N. Roberto de Barros, Y. Zhu, N. Engin Vrana, H. B. Kraatz, H.-J. Kim and A. Khademhosseini, Peptide Hydrogels as Immunomaterials and Their Use in Cancer Immunotherapy Delivery, *Adv. Healthcare Mater.*, 2023, 2301096.